ELSEVIER

Journal of Organometallic Chemistry 564 (1998) 71–79

Journal of Organometallic Chemistry

# Syntheses and properties of tetrathio- and tetraseleno metalates $[(C_5Me_4R)_2NbE_2]_2M$ (E = S, Se; M = Cr, Mo; R = Me, Et) with peripheric niobocene ligands

Olivier Blacque [b], Henri Brunner [a], Marek M. Kubicki [b], Dominique Lucas [b], Walter Meier [a], Yves Mugnier [b], Bernd Nuber [c], Bernhard Stubenhofer [a], Joachim Wachter [a,*]

[a] *Institut für Anorganische Chemie der Universität Regensburg, D-93040 Regensburg, Germany*
[b] *Laboratoire de Synthèse et d'Electrosynthèse Organométalliques, Université de Bourgogne, F-21100 Dijon, France*
[c] *Anorganisch-chemisches Institut der Universität Heidelberg, D-69120 Heidelberg, Germany*

Received 26 January 1998; received in revised form 1 April 1998

**Abstract**

Reactions of $Cp^*_2Nb(\eta^2\text{-}S_2)H$ **1** ($Cp^* = C_5Me_5$ (**a**), $C_5Me_4Et$ (**b**)) and $Cp^*_2Nb(\eta^2\text{-}Se_2H)$ **3** with 0.5 equivalents of $M(CO)_6$ (M = Cr, Mo) in boiling toluene give the CO free complexes $[Cp^*_2NbE_2]_2M$ **4–7**. X-ray diffraction analyses have been carried out for the Mo complexes **5a** (E = S) and **7a** (E = Se) showing that the structures contain $ME_4$ tetrahedral cores with two attached niobocene ligands thus forming a nearly linear trimetallic unit. Absorption spectra and electrochemical studies of complexes **4–7** are described. Characteristic of the novel $CrSe_4$ chromophor are four reversible one electron redox steps. Chemical oxidation of **4a** and **5a** with $[(C_5H_5)_2Fe]PF_6$ gives the salts $\{[Cp^*_2NbS_2]_2M\}PF_6$ (M = Cr, Mo) **10** and **11**. A qualitative EHMO analysis provides evidence for a strong delocalisation of electron density over the whole metal–ligand system. 

*Keywords:* Niobocene; Sulfur; Selenium; Polymetal complexes

## 1. Introduction

Trinuclear organometallic tetrathiometalates of the type $[L_nM']_2MS_4$ may be defined as compounds built up of a central $MS_4$ core which ligates two peripheric organometallic groups $L_nM'$ [1]. Corresponding to this description most of the syntheses employ anionic tetrathiometalates being available as stable salts e.g. $ReS_4^-$ or $MS_4^{2-}$ (M = Mo, W) [2] (Eq. 1). The related chemistry of selenometalates is much less developed [3]. Recently, we have described an alternative synthetic approach for tetrathiometalates employing starting materials in 'inversed' oxidation states [4]. This means that the central metal M arises from a binary metal carbonyl whereas the organometallic part as well as the sulphur ligands are provided by niobocene(V) hydrido sulfides, e.g. **1** (Eq. 2).

$$2\,L_nM'Cl + (Ph_4P)_2MS_4 \xrightarrow{-\,Ph_4PCl} [L_nM']_2MS_4 \quad (1)$$

$$\underset{\mathbf{1a}}{2\,Cp^*_2NbS_2H} + M_2(CO)_{8(9)} \xrightarrow{-CO,\,-H_2} \underset{\substack{\mathbf{2}\\ \mathbf{(M = Fe, Co)}}}{[Cp^*_2NbS_2]_2M} \quad (2)$$

In this study, we report on the preparation of tetrathio and tetraselenido metalates of Cr and Mo via

* Corresponding author. Fax: +49 941 9434439.

0022-328X/98/$19.00 
*PII* S0022-328X(98)00615-9

the metal carbonyl route and a comparative evaluation of some of their spectroscopic and electronic properties.

## 2. Results and discussion

### 2.1. Syntheses

Niobocene chalcogenides of composition $Cp^*_2NbE_2H$ ($Cp^* = C_5Me_5$ (**a**), $C_5Me_4Et$ (**b**)) exist in several isomeric forms. In the present case $Cp^*_2Nb(\eta^2\text{-}S_2)H$ [5] **1** and $Cp^*_2Nb(\eta^2\text{-}Se_2H)$ **3** [6] have been employed which lead to similar results in spite of the different nature of the ligands [7].

$$2\,[Cp^*_2NbCl] + (Ph_4P)_2MoS_4 \xrightarrow[>60°C]{DME} \underset{\mathbf{5}}{[Cp^*_2NbS_2]_2Mo} + 2\,Ph_4PCl \qquad (4)$$

Reactions of **1** or **3** with 0.5 equivalents of $M(CO)_6$ (M = Cr, Mo) in boiling toluene (Eq. 3a) give dark solutions from which the CO-free complexes **4** and **5** are obtained after column chromatography in yields from 12 to 87%. Complexes **6** and **7** are better prepared from THF solutions containing $M(CO)_5THF$ at 20°C (Eq. 3b). Analytical and mass spectroscopic data are consistent with formulas $Cp^*_4Nb_2E_4M$. IR and $^1H$-NMR spectra of **4–7** do not contain significant structural information. Although CO containing intermediates have been observed by IR spectroscopy, distinct products could not be isolated. Possible intermediate products may include $M(CO)_5$ adducts at the dichalcogenide ligands of **1** or **3**. Such adducts have been established under mild conditions in the case of **1** [8]. They thermally decompose to give **4** or **5** in moderate yields.

$$\underset{\mathbf{1}}{2\,Cp^*_2Nb(S_2)H} + M(CO)_6 \xrightarrow{\text{toluene, 115 °C}} [Cp^*_2NbS_2]_2M \quad \text{a)}$$
$$\mathbf{4}\ (M = Cr),\quad \mathbf{5}\ (M = Mo)$$

$$\underset{\mathbf{3}}{2\,Cp^*_2Nb(Se_2H)} + M(CO)_5THF \xrightarrow{\text{THF, 20 °C}} [Cp^*_2NbSe_2]_2M \quad \text{b)} \qquad (3)$$
$$\mathbf{6}\ (M = Cr),\quad \mathbf{7}\ (M = Mo)$$

Products identical with **5** in colour, analytical and spectroscopic properties are obtained from the reaction of $(Ph_4P)_2MoS_4$ with solutions of $Cp^*_2NbCl_2$ reduced with Na in dimethoxyethane (Eq. 4), which proceeds only at temperatures above 60°C. The reactive species in these solutions may be $Cp^*_2NbCl(DME)$ or '$Cp^*_2Nb$' according to the employed reduction equivalents [9]. Among several unidentified compounds the yellow complexes $[Cp^*_2NbS_2]_2Mo$ **5** are isolated in moderate yields (10–17%) and characterised by means of IR, $^1H$-NMR, and mass spectroscopy, as well as by X-ray diffraction analysis. It has been impossible to improve the yields of **5** by varying the ratio of the starting materials. Surprisingly, complex **5a** forms also in the reaction of $Cp^*_2NbCl_2$ with $(Ph_4P)_2MoS_4$, for in the case of the unsubstituted niobocene complex the dinuclear complex $(C_5H_5)_2NbMoS_4$ **8** has been obtained by this reaction [10]. Additionally, complex mixtures of compounds of higher nuclearity were found, again demonstrating the electron transfer capabilities of the system [11].

### 2.2. Molecular structures

X-ray structure analyses of **5a** and **7a** have been carried out. An almost linear Nb–Mo–Nb trimetallic arrangement, a distorted central $MoE_4$ tetrahedron, and mutually perpendicular niobocene units are the common features for both structures, as shown in Figs. 1 and 2. The geometries observed are similar to those found for $[(C_5H_5)_2NbS_2]_2Mo$ [12] and $[Cp^*_2NbS_2]_2Fe$ [4], leading to an approximate $D_{2d}$ molecular symmetry. The Nb – Mo distances of 3.049 Å (**5a**) and 3.166 Å (**7a**) (Table 1) may indicate weak metal–metal interactions. The metric parameters found for the central core of **5a** (mean Mo – S = 2.249 Å, mean Nb – S = 2.432 Å) are close to those reported for $[(C_5H_5)_2NbS_2]_2Mo$ [12]. The values observed for the selenium derivative **7a** reflect the difference of S versus Se covalent radii of 0.13 Å. The geometry of the central $MoSe_4$ core corresponds well to that reported for the $[(CN)_2Au_2MoSe_4]^{2-}$ anion ([3]b), the Mo – Se distances (mean 2.375 Å) being longer by 0.03 Å than in the gold anion. Because of the complexation of $MoSe_4^{2-}$ with niobocene fragments, the Mo – Se bonds in **7a** are also longer compared to those in the discrete $MoSe_4^{2-}$ ion (2.239 Å) [13].

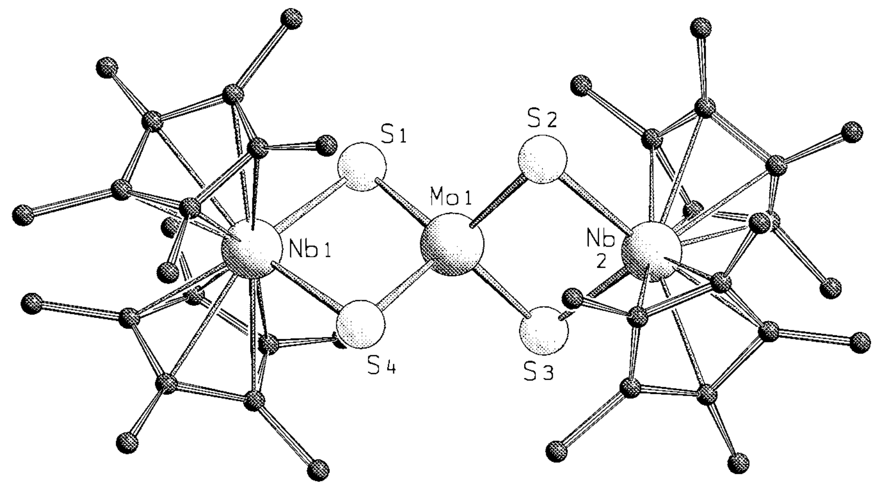


Fig. 1. Crystal structure of $[(C_5Me_5)_2NbS_2]_2Mo$ (**5a**) (Schakal plot).

*2.3. UV–vis spectroscopy and EHMO calculations*

The patterns of the UV–vis electronic spectra of the molybdenum complexes **5** and **7** are apparently similar to those observed for the discrete $MoS_4^{2-}$ and $MoSe_4^{2-}$ anions [14]. In particular, two very strong bands are recorded at 366 and 422 nm for **5a** and at 373 and 509 nm with a shoulder at 560 nm for **7a**. Additionally, very weak and broad bands are detected at 670 nm for **5a** and 710 nm for **7a**. These bands are absent in the spectra of discrete $MoS_4^{2-}$ anions [14,15] as well as in their thio complexes with closed shell $d^{10}$ metals ($Cu^I$, $Ag^I$) [16].

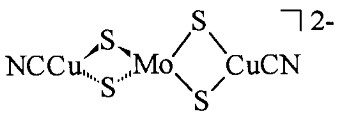

**9**

In order to understand the nature of the spectra we have carried out calculations at the extended Hückel level [17] on the hypothetical unsubstituted cyclopentadienyl complexes $[(C_5H_5)_2NbE_2]_2M$ (M = Cr, Mo; E = S, Se) as model compounds, on $MoE_4^{2-}$, and on the $[(CN)_2Cu_2MoS_4]^{2-}$ anion **9** [16]. The qualitative correlation energy diagram for these tetrathiometalates is shown in Fig. 3. It clearly demonstrates, in agreement with previous work [14,16], that the $\nu_1$ and $\nu_2$ bands observed for $ME_4^{2-}$ tetrahedra and in their complexes with $Cu^I$ and $Ag^I$ with $D_{2d}$ symmetry involve the $t_1$ and $3t_2$ filled levels and the empty 2e tetrahedral level. In contrast, coordination of niobocene fragments at the $ME_4^{2-}$ unit gives rise to quite different electronic structures. Thus, the original tetrahedral 2e and $4t_2$ orbitals split in $D_{2d}$ symmetry into the $4a_1$ and $2b_2$, and 5e and $4b_1$ levels, respectively. The $4a_1$ and $4b_1$ orbitals are strongly stabilized by interactions with niobocene lone pairs localized at the niobium atom [18]. These interactions lead to the formation of $12b_1$ and $12a_1$ molecular orbitals which consequently have a metallic (d, predominant Nb) nature. Higher energy molecular orbitals LUMO ($7b_2$) and LUMO + 1 (18e) have a major contribution from the $MoS_4^{2-}$ unit and are mostly built up of molybdenum atomic orbitals. The lower energy molecular orbitals (17e, $6a_2$, 16e...) are principally formed by combinations in which cyclopentadienyl rings and sulphur atoms are involved. Consequently, they are of 'p' nature. This qualitative energy diagram may explain the nature of electronic transitions observed for our complexes. The very weak low energy bands are due to the d–d (Nb–Mo) transitions involving the HOMO's ($12a_1$, $12b_1$) and the LUMO's ($7b_2$, 18e), while the strong higher energy bands are of charge transfer p–d nature involving transitions between the molecular orbitals derived from cyclopentadienyl carbons (13e and 12e) and sulphur ($t_1$ and $3t_2$) with metallic LUMO's ($7b_2$ and 18e). The exact composition of excited states and, consequently, the energy of transitions cannot be calculated because the extended Hückel approximation is unable to treat the configuration interaction.

It is worth noting that in the copper complex the levels $8a_1$ and $8b_1$ (Fig. 3) principally formed by both Cu(CN) fragments have energies very close to those resulting from the contribution of the tetrasulphur unit (tetrahedral $t_1$). Consequently, the hypothetical electronic transitions involving these levels may be hidden by the charge transfer bands in the $MoS_4$ core. Contrary to the niobium complexes the $9a_1$ and $3b_2$ LUMO's (tetrahedral 2e) have no significant contribution from copper.

The spectra of the chromium complexes **4** and **6** exhibit three significant bands and it is striking that the low energy absorption of **4a** at 705 nm is much stronger than that in the molybdenum analogue. This may sug-

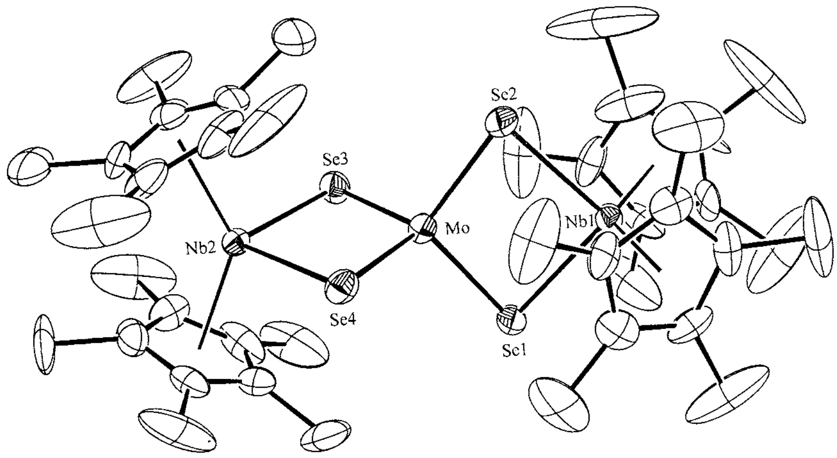


Fig. 2. Crystal structure of $[(C_5Me_5)_2NbSe_2]_2Mo$ (**7a**). ORTEP plot at the 30% probability level.

Table 1
Selected bond lengths (Å) and angles (°) of $[(C_5Me_5)_2NbE_2]_2Mo$ (E = S: **5a**; E = Se: **7a**)

| | E = S (**5a**) | E = Se (**7a**) |
|---|---|---|
| Bond length (Å) | | |
| Mo–E(1) | 2.252(4) | 2.370(2) |
| Mo–E(2) | 2.256(6) | 2.376(2) |
| Mo–E(3) | 2.240(5) | 2.378(2) |
| Mo–E(4) | 2.255(5) | 2.379(2) |
| Nb(1)–E(1) | 2.431(5) | 2.575(2) |
| Nb(1)–E(2) | 2.425(5) | 2.570(2) |
| Nb(2)–E(3) | 2.434(5) | 2.570(2) |
| Nb(2)–E(4) | 2.431(5) | 2.562(2) |
| Nb(1)...Mo | 3.045(3) | 3.168(2) |
| Nb(2)...Mo | 3.052(3) | 3.156(2) |
| Bond angle (°) | | |
| Nb(1)–Mo–Nb(2) | 176.0(1) | 176.2(1) |
| E(1)–Mo–E(2) | 112.9(2) | 105.9(1) |
| E(1)–Mo–E(3) | 113.2(2) | 111.2(1) |
| E(1)–Mo–E(4) | 103.9(2) | 111.3(1) |
| E(2)–Mo–E(3) | 103.9(2) | 112.5(1) |
| E(2)–Mo–E(4) | 112.3(2) | 110.0(1) |
| E(3)–Mo–E(4) | 110.8(2) | 106.0(1) |
| E(1)–Nb(1)–E(2) | 93.9(2) | 94.9(1) |
| E(3)–Nb(2)–E(4) | 93.4(2) | 95.4(1) |
| Mo–E(1)–Nb(1) | 81.0(1) | 79.6(1) |
| Mo–E(2)–Nb(1) | 81.1(1) | 79.5(1) |
| Mo–E(3)–Nb(2) | 81.5(2) | 79.2(1) |
| Mo–E(4)–Nb(2) | 81.1(2) | 79.3(1) |

gest that the composition of MO's involved in the electronic transitions and the distortion of the $ME_4$ cores are different in Cr and Mo compounds. It can be due to different atomic sizes of these metals. Unfortunately, in spite of numerous attempts, we were not able to obtain diffracting crystals of **4** or **6**.

It should be mentioned here that the simple model of bonding in complexes **4**–**7** agrees with electrochemical data (vide infra). In particular, the energies of the HOMO's vary little as do the first oxidation potentials, and there is roughly linear correlation between the first reduction potentials with the energies of the LUMO's.

### 2.4. Cyclovoltammetric studies

The electrochemical behaviour of complexes **4**–**7** has been studied (Table 2). As a common feature all investigated compounds are easily oxidised, for their first oxidation potential is in the same range of about 0 V. So the corresponding electron transfer should take place in a structural unit common to all complexes, e.g. the $[Cp^*_2Nb^{III}]^+$ fragment if the valence bond formalism is used (Eq. 5a). Indeed, a close oxidation potential has been found for the related mononuclear complex $[C_5H_4SiMe_3)_2Nb^{III}(THF)]^+$ [19].

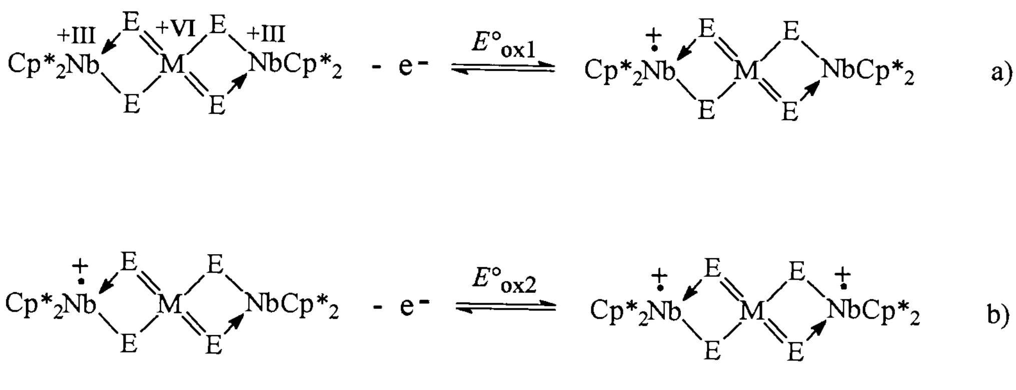


(5)

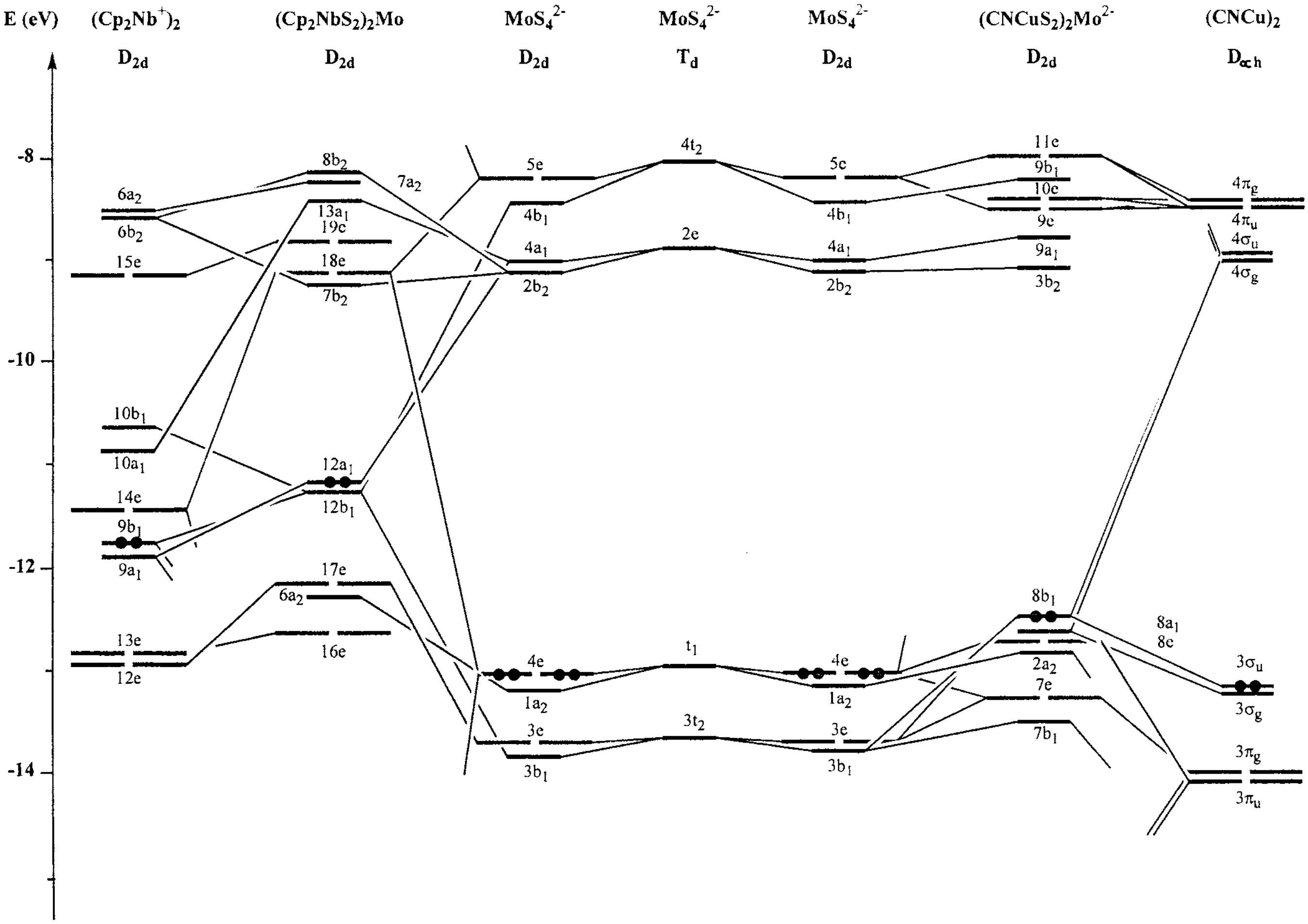


Fig. 3. Correlation energy diagram for $[(C_5H_5)_2NbS_2]_2Mo$, $MoS_4^{2-}$ and $[(NC)_2Cu_2MoS_4]^{2-}$ (**9**).

For each complex a second oxidation step is located in the potential range of 0.7 V. It may be tentatively ascribed to the oxidation of the second $[Cp_2^*Nb^{III}]^+$ fragment so that the overall oxidation process can be described by the two successive one-electron transfer reactions given in Eq. 5.

The difference between the half-wave potentials (nearly 0.7 V) denotes a strong mutual interaction between the two Nb atoms. Many dinuclear species display redox activity in solution disclosing two consecutive one-electron redox steps. The separation of the potentials associated with each redox event may reach several hundreds of millivolts for complexes in which a large electronic interaction exists between both metal centres [20]. In our case the $ME_4$ bridging unit seems to favour the communication between the two Nb atoms.

In contrast to the oxidation processes the first reduction potentials of **4–7** are susceptible to the nature of the central metals and chalcogenes, for they vary from − 1.385 to − 2.30 V (on Hg electrode). Substitution of sulphur by selenium induces a shift towards more positive values (**4b** → **6b**: 145 mV; **5b** → **7b**: 230 mV on Hg electrode). The second reduction potentials are only reversible in the case of the $CrSe_4$ complex **6b**, which is the only compound exhibiting four reversible one-electron steps (Fig. 4).

Complexes **4–7** have closed valence shells and are therefore diamagnetic, so one electron reduction or oxidation should lead to paramagnetic species. All monocations are EPR silent, but spectra have been obtained for the reduced forms of **4b** and **6b** in spite of their high sensitivity to air. Both monoanions exhibit 19 lines spectra (Fig. 5) with similar $g$ values and $A_{Nb}$ coupling constants **4b**: $g_{iso} = 1.9855$, $a_{iso} = 19.4$ G; **6b**: $g_{iso} = 2$, $a_{iso} = 17.3$ G). The complex pattern may be explained by interaction of the unpaired electron spin with the two Nb centres, indicating its strong delocalisation over the whole trimetallic system including the chalcogene ligands. Hyperfine structures due to coupling with $^{53}Cr$ or $^{77}Se$ cannot be detected.

In agreement with the electrochemical results chemical oxidation of **4a** and **5b** by means of $[(C_5H_5)_2Fe]PF_6$ leads to the corresponding $PF_6$ salts **10** and **11**. Their electronic spectra in the visible region exhibit similar patterns as the neutral compounds, but with drastically increased intensities of the maxima.

Table 2
Electrochemical data and energies (eV) of HOMO and LUMO molecular orbitals for complexes **4**–**7**[a]

| Complex | $E^{b}_{1/2,\,ox2}$ | $E_{1/2,\,ox1}$ | $E_{1/2,\,red1}$ | $E_{1/2,\,red2}$ | $\Delta E_{1/2}$(ox2-ox1) | $\Delta E_{1/2}$(ox1-red1) | HOMO[e] | LUMO[e] |
|---|---|---|---|---|---|---|---|---|
| **4a** | +0.69 (+0.75) | −0.025 (+0.045)[b] | −1.535 (−1.44) | −2.72 (irr.; $E_p \approx -2.7$) | 0.715 (0.715) | 1.51 (1.485) | — | — |
| **4b** | +0.69 (+0.75) | −0.03 (+0.04) | −1.53 (−1.46) | −2.68 (irr.; $E_p$: −2.7) | 0.72 (0.71) | 1.495 (1.50) | −11.405 (12a1) | −10.044 (7b2) |
| **5a** | +0.69 (+0.78) | −0.02 (+0.05) | −2.11 (−2.00) | —[c] | 0.71 (0.73) | 2.09 (2.05) | — | — |
| **5b** | +0.77 (+0.81) | +0.01 (+0.055) | ≈−2.20[d] (−1.98) | —[c] | 0.76 (0.755) | 2.21 (2.035) | −11.506 (12a1) | −9.216 (7b2) |
| **6b** | +0.7 (+0.64) | −0.035 (−0.03) | −1.385 (−1.37) | −2.29 (−2.24) | 0.735 (0.67) | 1.42 (1.40) | −11.506 (12b1) | −10.306 (7b2) |
| **7b** | +0.675 (+0.775) | −0.035 (+0.07) | −1.97 (−1.85) | —[c] | 0.71 (0.705) | 2.005 (1.92) | −11.275 (12b1) | −9.412 (7b2) |

[a] The potentials (V) are relative to saturated aqueous calomel electrode (+0.248 V/ENH). [b] $E_{1/2}$ determined on Hg (or carbon) electrodes. [c] Not observed. [d] Ill-defined. [e] Values for model $(C_5H_5)$ complexes.

In conclusion, syntheses of organometallic tetrathio- and tetraselenometalates are described, in which the central 'inorganic' part arises from a binary transition metal carbonyl, thus permitting access to the novel $CrE_4$ chromophor in a complex redox reaction. This alternative synthetic route complements the conventional metathesis route, in which $ME_4$ units are already preformed as central building blocks. By means of the Mo complex **5** it has been shown that both methods lead to identical products independent of the initial oxidation numbers of the starting materials. These findings along with electronic, spectroscopic and electrochemical characteristics are indicative of a strongly delocalised bonding system, and they are supported by EHMO analyses of hypothetic $[(C_5H_5)_2NbS_2]_2M$ complexes.

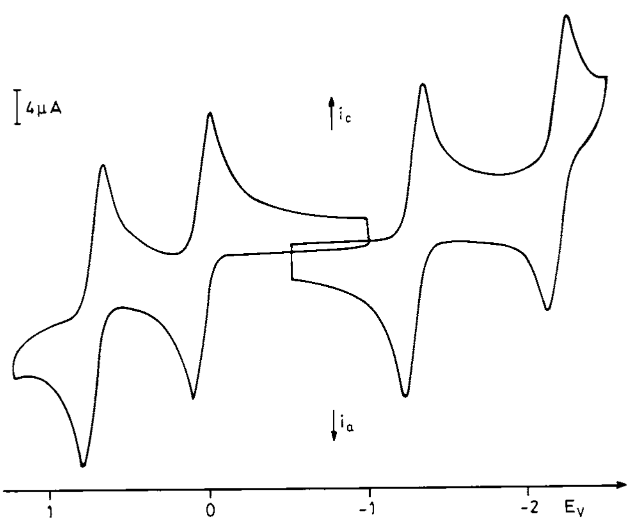


Fig. 4. Cyclic voltammogram of **6b** in a 0.2 M solution of $n$-$Bu_4NPF_6$ in THF. Starting potential: −0.5 V (cathodic scan) and −1 V (anodic scan). Sweep rate: 0.1 V $s^{-1}$.

## 3. Experimental section

Experimental and spectroscopic techniques as well as the preparation of $Cp^*_2NbS_2H$ **1a,b** are reported in ref. [5]. $Cp^*_2NbSe_2H$ **3** is prepared from $Cp^*_2NbBH_4$ and Se in the dark [6]. The synthesis of $(Ph_4P)_2MoS_4$ is described in ref. [11].

Voltammetric analyses were carried out in a standard three-electrode cell with a Tacussel UAP4 unit. The reference electrode was a saturated calomel electrode separated from the solution by a sintered glass disk. The auxiliary electrode was a Pt wire. For all voltammetric measurements, the working electrode was a vitreous carbon disk electrode. For the polarograms, a three-electrode Tacussel Tipol polarograph was used. The dropping Hg electrode characteristics were $m = 3$ mg $s^{-1}$ and $E = 0.5$ s. The controlled potential electrolysis were performed with an Amel 552 potentiostat coupled to an Amel 721 electronic integrator. In all cases the electrolyte was a 0.2 M solution of $^{n}Bu_4NPF_6$ in THF.

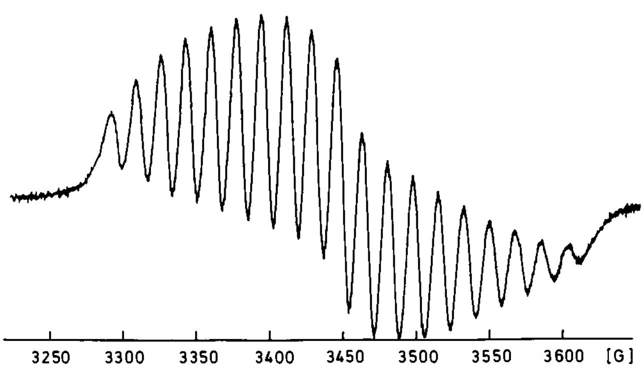


Fig. 5. EPR spectrum for reduced $[(C_5Me_4Et)_2NbS_2]_2Cr$ (**4b**): Solvent THF, $a_{iso} = 16.107$ G, $g_{iso} = 1.9847$.

### 3.1. Synthesis of $[Cp^*_2NbS_2]_2Cr$ **4a,b**

A mixture of 0.5 mmol $Cp^*_2NbS_2H$ (**1a,b**), 0.25 mmol $Cr(CO)_6$, and 50 ml of toluene was refluxed for 72 (**4a**) or 16 h (**4b**), giving a red solution. After cooling to room temperature (r.t.) the solvent was evaporated, the residue dissolved in 10 ml of toluene and chromatographed on $SiO_2$ (column 15 × 3 cm). Elution with toluene gave a pale yellow band which was discarded and then a dark red band containing $[Cp^*_2NbS_2]_2Cr$ in 18.8 (**4a**) or 87% (**4b**) yield. The compounds were recrystallised from toluene:pentane (1:1) at −20°C.

**4a**: Anal. Found: C, 53.24; H, 6.62, $C_{40}H_{60}CrNb_2S_4$ (906.9). Calc.: C, 52.97; H, 6.62%. FD-MS (from toluene): 906.2. $^1$H-NMR (250 MHz, $CDCl_3$): 2.03 ppm. UV ($CH_2Cl_2$): ε(318 nm(sh)) = 13158, ε(406 nm) = 17429, ε(540 nm) = 6143, ε(705 nm) = 5296 $M^{-1}cm^{-1}$.

**4b**: Anal. Found: C, 54.93; H, 7.13, $C_{44}H_{68}CrNb_2S_4$ (963.0). Calc.: C, 54.93; H, 7.12%. FD-MS (from toluene): 963.1. $^1$H-NMR (250 MHz, $CDCl_3$): 1.82 (s, 24H, $CH_3$), 1.74 (s, 24H, $CH_3$), 0.91 (t, 12H, $CH_3$), 2.28 (q, 8H, $CH_2$) ppm. UV ($CH_2Cl_2$): ε(312 nm(sh)) = 16484, ε(409 nm) = 18315, ε(542 nm) = 6623, ε(700 nm) = 4836 $M^{-1}$ $cm^{-1}$.

### 3.2. Synthesis of $[Cp^*_2NbS_2]_2Mo$ **5a,b**

#### 3.2.1. Method A

A mixture of 1.0 mmol of $Cp^*_2NbS_2H$ (**1a,b**), 0.5 mmol of $Mo(CO)_6$, and 50 ml of toluene was refluxed for 18 h. The colour of the solution turned from orange to green (after 10 min) and finally brown–green. After cooling the solvent was evaporated, the residue dissolved in 15 ml of toluene and chromatographed on silica gel (column 20 × 3 cm). With toluene a yellow–brown band was eluted which was further purified by an additional chromatography ($SiO_2$, toluene:pentane (2:1) as eluent). Yellow bands were isolated containing **5a** in 15% and **5b** in 12% yield. Recrystallisation was carried out using toluene.

#### 3.2.2. Method B

A suspension of 0.5 mmol of **1a,b** in 50 ml of dimethoxyethane was reduced with three equivalents of Na (in 10 ml of Hg) [9]. After 60 min the solution was decanted and 0.25 mmol of $(Ph_4P)_2MoS_4$ were added. After stirring for 60 min at 65°C the mixture was filtered, the solvent evaporated and the residue transferred onto the top of a column ($SiO_2$, 15 × 3 cm). With toluene a yellow band was eluted containing **5a,b** in yields between 10 and 17%.

**5a**: Anal. Found: C, 50.37; H, 6.11, $C_{40}H_{60}MoNb_2S_4$ (950.8). Calc.: C, 50.53; H, 6.31%. FD-MS (from toluene): 946.3 ($^{92}$Mo). $^1$H-NMR (250 MHz, $CDCl_3$): 1.99 ppm. UV ($CH_2Cl_2$): ε(366 nm) = 13278, ε(422 nm) = 8798, ε(670 nm) = 300 $M^{-1}$ $cm^{-1}$.

**5b**: Anal. Found: C, 52.73; H, 6.82, $C_{44}H_{68}MoNb_2S_4$ (1006.9). Calc.: C, 52.48; H, 6.76%. FD-MS (from toluene): 1002.5 ($^{92}$Mo). $^1$H-NMR (250 MHz, $CDCl_3$): 1.90 (s, 24H, $CH_3$), 1.93 (s, 24H, $CH_3$), 0.87 (t, 12H, $CH_3$), 2.30 (q, 8H, $CH_2$) ppm. UV ($CH_2Cl_2$): ε(343 nm) = 12990, ε(449 nm) = 11237 $M^{-1}$ $cm^{-1}$.

### 3.3. Syntheses of $[Cp^*_2NbSe_2]_2M$ (M = Cr (**6**), Mo (**7**))

A mixture of 0.5 mmol of $Cp^*_2NbSe_2H$ (**3a,b**) and two equivalents of $Cr(CO)_5THF$ in 150 ml of THF was stirred in the dark for 72 h at r.t. After evaporation of the solvent the green–brown residue was dissolved in 15 ml of toluene and chromatographed on $SiO_2$ (column 15 × 3 cm). With toluene green (**6a,b**) or red–brown (**7a,b**) bands were eluted. The yields were 39% for $[(C_5Me_5)_2NbSe_2]_2Cr$ **6a**, 36% for $[(C_5Me_4Et)_2NbSe_2]_2Cr$ **6b**, 67% for $[(C_5Me_5)_2NbSe_2]_2Mo$ **7a** and 61% for $[(C_5Me_4Et)_2NbSe_2]_2Mo$ **7b**, respectively.

**6a**: Anal. Found: C, 43.68; H, 5.21, $C_{40}H_{60}CrNb_2Se_4$ (1094.5). Calc.: C, 43.89, H, 5.52%. FD-MS (from toluene): 1095.1 (centre). $^1$H-NMR (250 MHz, $C_6D_6$): 1.93 ppm. UV ($CH_2Cl_2$): ε(307 nm) = 16945, ε(439 nm) = 5128, ε(613 nm) = 2537, ε(879 nm) = 2486 $M^{-1}$ $cm^{-1}$.

**6b**: Anal. Found: C, 45.97; H, 5.81, $C_{44}H_{68}CrNb_2Se_4$ (1150.9). Calc.: C, 45.93; H, 5.93%. FD-MS (from toluene): 1151.1 (centre). $^1$H-NMR (250 MHz, $C_6D_6$): 1.94 (s, 24H, $CH_3$), 1.97 (s, 24H, $CH_3$), 2.33 (q, 8H, $CH_2$), 0.85 (t, 12H, $CH_3$) ppm. UV ($CH_2Cl_2$): ε(309 nm) = 17297, ε(445 nm) = 5046, ε(610 nm) = 2346, ε(884 nm) = 2476 $M^{-1}$ $cm^{-1}$.

**7a**: Anal. Found: C, 42.44; H, 5.20, $C_{40}H_{60}MoNb_2Se_4$ (1138.5). Calc.: C, 42.20; H 5.31%. FD-MS (from toluene): 1138.9 (centre). $^1$H-NMR (250 MHz, $C_6D_6$): 1.86 ppm. UV ($CH_2Cl_2$): ε(317 nm) = 22523, ε(373 nm) = 31011, ε(509 nm) = 19987, ε(550 nm) = 6000 (shoulder), ε(710 nm) = 2000 $M^{-1}$ $cm^{-1}$.

**7b**: Anal. Found: C, 44.62; H, 5.91, $C_{44}H_{68}MoNb_2Se_4$ (1195.0). Calc.: C, 44.24; H, 5.74%. FD-MS (from toluene): 1195.0 (centre). $^1$H-NMR (250 MHz, $C_6D_6$): 2.22 (s, 24H, $CH_3$), 2.26 (s, 24H, $CH_3$), 2.70 (q, 8H, $CH_2$), 0.87 (t, 12H, $CH_3$) ppm. UV ($CH_2Cl_2$): ε(323 nm) = 23003, ε(377 nm) = 30834, ε(511 nm) = 18945 $M^{-1}$ $cm^{-1}$.

### 3.4. Preparation of $\{[Cp^*_2NbS_2]_2M\}PF_6$ (M = Cr (**10**), Mo (**11**))

Equimolar mixtures (0.16 mmol) of **4a** or **5a** and $[(C_5H_5)_2Fe]PF_6$ in 100 ml of THF were stirred at r.t. for 20 h while the colour changed from red to green–brown (**4a**) or from yellow to dark red (**5a**). After evaporation of the solvent the residue was dissolved in

7 ml each of toluene and $CH_2Cl_2$ and filtered over a short column (5 cm) filled with $SiO_2$. Complexes **10** and **11** were eluted with $CH_2Cl_2$ in 87 and 51% yield, respectively, and recrystallised from $CH_2Cl_2$:pentane (1:1).

**10**: Anal. Found: C, 44.79; H, 5.83, $C_{40}H_{60}CrF_6PNb_2S_4$ (1051.0). Calc.: C, 45.67; H, 5.57%. FD-MS (from $CH_2Cl_2$): 906.0 (cation calc. 906.0). UV ($CH_2Cl_2$): $\varepsilon$(351 nm) = 52287, $\varepsilon$(411 nm) = 51831, $\varepsilon$(438 nm(sh)) = 44541, $\varepsilon$(525 nm) = 16073$\varepsilon$, $\varepsilon$(700 nm) = 14836 $M^{-1}$ $cm^{-1}$.

**11**: Anal. Found: C, 43.36; H, 5.55, $C_{40}H_{60}F_6MoPNb_2S_4$ (1091.0). Calc.: C, 43.84; H, 5.52%. FD-MS (from $CH_2Cl_2$): 946.0 ($^{92}$Mo; cation calc. 950.8). UV ($CH_2Cl_2$): $\varepsilon$(325 nm) = 27315, $\varepsilon$(477 nm) = 14110, $\varepsilon$(690 nm) = 1700 $M^{-1}$ $cm^{-1}$.

### *3.5. Crystallographic data for **5a***

$C_{40}H_{60}Nb_2MoS_4 \cdot C_7H_8$, orthorhombic $D_2^4$, $P2_12_12_1$ (no. 19); cell: $a = 10.730(5)$, $b = 13.214(7)$, $c = 33.26(2)$ Å, $V = 4715.8$ Å$^3$, $Z = 4$; empirical absorption correction: five reflections $7.0 < 2\theta < 25.0°$. Transmission factors (min/max) 0.79/1.00, $D_{calc.} = 1.471$ g cm$^{-3}$, $\mu = 0.95$ mm$^{-1}$. Intensity data were measured on a Syntex R3 diffractometer. Mo–$K_\alpha$ radiation, graphite monochromator, 6826 unique observed reflections, 3333 independent reflections ($I \geq 2.2\sigma(I)$). Structure solution by Patterson and difference Fourier methods. All H atoms except those of the slightly disordered toluene were included in calculated positions. $R = 0.053$, $wR_2 = 0.040$; highest peak in difference Fourier 0.74 e Å$^{-3}$.

### *3.6. Crystallographic data for **7a***

$C_{40}H_{60}Nb_2MoSe_4 \cdot C_7H_8$, orthorhombic $D_2^4$, $P2_12_12_1$ (no. 19); cell: $a = 10.668(1)$, $b = 13.317(2)$, $c = 33.653(4)$ Å, $V = 4781.3$ Å$^3$, $Z = 4$; empirical absorption correction: seven reflections $6.0 < 2\theta < 24°$. Transmission factors (min/max) 0.93/0.95, $D_{calc.} = 1.711$ g cm$^{-3}$, $\mu = 37.485$ cm$^{-1}$. Intensity data were measured on an Enraf-Nonius CAD4 diffractometer. Mo–$K_\alpha$ radiation, graphite monochromator, 5141 unique observed reflections, 2825 independent reflections ($I \geq 2\sigma(I)$). Structure solution by Patterson and difference Fourier methods. All H atoms (except toluene) were included in calculated positions. Refinement on $F^2$. $R = 0.047$, $wR_2 = 0.092$; highest peak in difference Fourier 0.65 e Å$^{-3}$, GOF = 1.02; absolute structure parameter = 0.03(2).

## 4. Supplementary material available

Crystallographic data of **5a** and **7a** (excluding structure factors) have been deposited with the Cambridge Crystallographic Data Centre as supplementary publication no. CCDC-101348. Copies of the data can be obtained free of charge on application to The Director, CCDC, 12 Union Road, Cambridge CB2 1EZ, UK (Fax: +44 1223 336033; e-mail: deposit@chemcrys.cam.ac.uk).

## Acknowledgements

We are grateful to the Deutsche Forschungsgemeinschaft for support of this work. Parts of this work have been supported by the Deutscher Akademischer Austauschdienst and the Ministère des Affaires Etrangères (Procope program).

## References

[1] (a) K.E. Howard, T.B. Rauchfuss, A.L. Rheingold, J. Am. Chem. Soc. 108 (1986) 297. (b) P.A. Shapley, Z. Gebeyehu, N. Zhang, S.R. Wilson, Inorg. Chem. 32 (1993) 5646.

[2] (a) J.A. Kovacs, J.K. Bashkin, R.H. Holm, J. Am. Chem. Soc. 107 (1985) 1785. (b) L.D. Rosenheim, J.W. McDonald, Inorg. Chem. 26 (1987) 3414. (c) K.E. Howard, T.B. Rauchfuss, S.R. Wilson, Inorg. Chem. 27 (1988) 3561. (d) K.E. Howard, J.R. Lockemeyer, M.A. Massa, T.B. Rauchfuss, S.R. Wilson, X. Yang, Inorg. Chem. 29 (1990) 4385. (e) M. Kato, M. Kawano, H. Taniguchi, M. Funaki, H. Moriyama, T. Sato, K. Matsumoto, Inorg. Chem. 31 (1992) 26. (f) R. Schäfer, W. Kaim, J. Fiedler, Inorg. Chem. 32 (1993) 3199. (g) R. Schäfer, J. Fiedler, M. Moscherosch, W. Kaim, J. Chem. Soc. Chem. Commun. (1993) 896. (h) G. Sanchez, F. Momblana, G. Garcia, G. López, E. Pùrilla, A. Monge, J. Chem. Soc. Dalton Trans. (1994) 2271. (i) S. Ogo, T. Suzuki, K. Isobe, Inorg. Chem. 34 (1995) 1304. (j) Y. Mizobe, M. Hosomizu, Y. Kubota, M. Hidai, J. Organomet. Chem. 507 (1996) 179.

[3] (a) K.E. Howard, T.B. Rauchfuss, S.R. Wilson, Inorg. Chem. 27 (1988) 1710. (b) R.J. Salm, A. Misetic, J.A. Ibers, Inorg. Chim. Acta 240 (1995) 239.

[4] H. Brunner, M.M. Kubicki, G. Gehart, E. Lehrl, D. Lucas, W. Meier, Y. Mugnier, B. Nuber, B. Stubenhofer, J. Wachter, J. Organomet. Chem. 510 (1996) 291.

[5] (a) H. Brunner, U. Klement, J. Wachter, M. Tsunoda, J.-C. Leblanc, C. Moise, Inorg. Chem. 29 (1990) 584. (b) H.J. Bach, H. Brunner, J. Wachter, M.M. Kubicki, J.-C. Leblanc, F. Volpato, B. Nuber, M.L. Ziegler, Organometallics 11 (1992) 1403. (c) H. Brunner, G. Gehart, W. Meier, J. Wachter, B. Nuber, J. Organomet. Chem. 454 (1993) 117.

[6] B. Stubenhofer, Ph.D. Thesis, Universität Regensburg, 1997.

[7] Whereas the disulfido–hydrido arrangement dominates in complexes **1** in **3**, the hydrogen is attached to the chalcogene ligand. This unique coordination mode closely relates to that found in $Cp_2^*Nb(Te_2H)$ (O. Blacque, H. Brunner, M.M. Kubicki, B. Nuber, B. Stubenhofer, J. Wachter, B. Wrackmeyer, Angew. Chem. Int. Ed. Engl. 36 (1997) 352).

[8] H. Brunner, G. Gehart, J.-C. Leblanc, C. Moise, B. Nuber, B. Stubenhofer, F. Volpato, J. Wachter, J. Organomet. Chem. 517 (1996) 47.

[9] (a) H. Brunner, G. Gehart, W. Meier, J. Wachter, A. Riedel, S. Elkrami, Y. Mugnier, B. Nuber, Organometallics 13 (1994) 134. (b) H. Brunner, G. Gehart, W. Meier, J. Wachter, T. Burgemeister, J. Organomet. Chem. 493 (1995) 163.

[10] (a) G.J.S. Adams, M.L.H. Green, J. Organomet. Chem. 208 (1981) 299. (b) T.B. Rauchfuss, C.J. Ruffing, Organometallics 1 (1982) 400.
[11] A.I. Hadjikyriacou, D. Coucouvanis, Inorg. Synth. 27 (1990) 39.
[12] P.M. Boorman, J.F. Fait, G.K.W. Freeman, Polyhedron 8 (1989) 1762.
[13] S.C. O'Neal, J.W. Kolis, J. Am. Chem. Soc. 110 (1988) 1971.
[14] A. Müller, E. Diemann, R. Jostes, H. Bögge, Angew. Chem. Int. Ed. Engl. 20 (1981) 934.
[15] J. Bernholc, E.I. Stiefel, Inorg. Chem. 24 (1985) 1323.
[16] S.F. Geller, T.W. Hamblay, J.R. Rodgers, R.T.C. Brownlee, M.J. O'Connor, M.R. Snow, A.G. Wedd, Inorg. Chem. 23 (1984) 2519.
[17] (a) R.J. Hoffmann, J. Chem. Phys. 39 (1963) 1397. (b) C. Mealli, D.M. Proserpio, J. Chem. Educ. 67 (1990) 399. The metric parameters used for Mo complexes were taken from X-ray data.
[18] J.W. Lauher, R.J. Hoffmann, J. Am. Chem. Soc. 98 (1976) 1729.
[19] H. Nabaoui, Y. Mugnier, A. Fakhr, F. Laviron, A. Antiñolo, F.A. Jalon, M. Fajardo, A. Otero, J. Organomet. Chem. 375 (1989) 67.
[20] M. Ciampolini, L. Fabrizzi, A. Perrotti, A. Poggi, B. Seghi, F. Zanobini, Inorg. Chem. 26 (1987) 3527.